A wear model for assessing the reliability of wave energy converter in heave with hydraulic power take-off

L. M. Yang[1], J. Hals[2] and T. Moan[3]

[1]Centre for Ships and Ocean Structures (CeSOS),
Norwegian University of Science and Technology (NTNU),
Otto Nielsens V.10, N-7491, Trondheim, Norway
E-mail: limin.yang@ntnu.no

[2]Centre for Ships and Ocean Structures (CeSOS),
Norwegian University of Science and Technology (NTNU),
Otto Nielsens V.10, N-7491, Trondheim, Norway
E-mail: jorgen.hals@ntnu.no

[3]Centre for Ships and Ocean Structures (CeSOS),
Norwegian University of Science and Technology (NTNU),
Otto Nielsens V.10, N-7491, Trondheim, Norway
E-mail: torgeir.moan@ntnu.no

Abstract

Understanding and managing the safety and reliability issues of ocean energy converters is a key factor in the development of viable technologies. This requires mathematical models that enable numerical solution with the sufficient accuracy and computational efficiency. In this study a point absorber has been chosen as an example of a wave energy converter (WEC). The converter has been modelled by using bond graphs – a systematic and useful method for systems spanning several energy domains.

In the hydraulic system of the WEC, the piston ring and cylinder play very important roles in achieving desired energy converting performance and durability. In this paper, an abrasive wear model for the piston ring and cylinder is developed during the steady state operation by using the Archard's abrasive wear equation. Based on time domain simulation results for the full conversion system, the development of wear in the piston ring is modelled as a function of the contact pressure and relative motion. The procedure to determine the time to failure due to the scuff for the ring is calculated for a case with one sea state only.

Keywords: bond graph, abrasive wear, wave energy converter, piston ring , hydraulic piston pump

Nomenclature

β = bulk modulus
μ = friction coefficient
η = kinematic viscosity of the oil
γ = ratio of specific heat
ρ = oil density
ω = angular frequency
υ = mean frequency
A = area
$\tilde{\mathbf{A}}, \tilde{\mathbf{B}}, \tilde{\mathbf{C}}, \tilde{\mathbf{D}}$ = state-space matrices
B = damping coefficient
c = discharge coefficient
C = restoring coefficient
d = ring thickness
D = diameter
$E[s]$ = mean value of s
$f_s(s)$ = the probability density of s
F = force
h = wear depth
H_s = significant wave height
k = steepness of Coulomb friction curve
K = wear constant
$K(t)$ = the retardation function
m = added mass
M = mass
N = normal load
N_T = total number of cycles in the time interval T_f
p = contact pressure
P = fluid pressure
Q = fluid volume
R = Reynolds number
Rou = roughness (centre line average)
s = motion amplitude
t = time
T_2 = mean wave period
T = time interval of the motion
v = velocity
V = geometric volume
V_w = wear volume
w = ring width
WEC = wave energy converter
x = sliding distance
X = motion coordinate
$\mathbf{z}$ = additional state-space vector

Subscripts

0	=	initial or default value
∞	=	infinite frequency
acc	=	accumulator
c	=	Coulomb friction
con	=	contact
d	=	discharge
exc	=	exciting force
ext	=	external force
n	=	normal direction
net	=	net flow
R	=	radiation
s	=	static friction
st	=	Stribeck character
turb	=	turbulent flow
v	=	viscous friction
val	=	valve
w	=	wear

1 Introduction

Ocean wave is a non-polluting and renewable source of energy, created by natural conversion of part of the wind blowing over the oceans. Various types of wave energy converters (WEC) are currently under development, and most of them are planned for electricity production. In the present work an oil-hydraulic system is used in the secondary step in energy conversion for a heaving wave energy absorber. The main devices include an absorber, an oil-hydraulic system, a hydraulic motor and a generator. A simplified diagram of the absorber and its connection to the hydraulic cylinder is shown in Fig. 1 (a more detailed description can be found in [1]). Fig. 2 shows the hydraulic system for a single absorber which is connected to the motor and generator.

In the hydraulic system of the WEC, the piston ring and cylinder play very important roles in achieving the desired energy conversion performance and durability. The rings are used to seal the clearance between the cylinder and the piston in order to retain the operating pressure in the cylinder. In addition, the reciprocating piston-rod seal is another critical element in this hydraulic component. A leaking rod seal can cause operational problems and environmental pollution. Hence it is important for designers and users to have knowledge about the seal durability. The detailed diagram of the sealed hydraulic system is shown in Fig. 3.

One of the important causes of leakage for the hydraulic system is the wear. A number of studies in the past indicated that the wear in the interface between the ring seals and the cylinder bore progress in stages. Initially, wear increases rapidly with time due to running-in and then attains a steady state period. For the hydraulic system, it spends most of its useful life in the steady state period. During this period, abrasive wear is generally considered to be a dominant wear mechanism for the piston ring and cylinder bore [2-4]. In this work, an abrasive wear model for the piston ring is developed based on the Achard's equation [5].

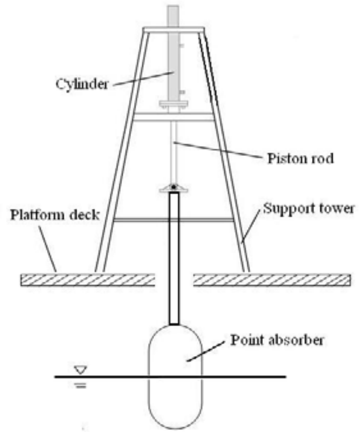

Figure 1: A heaving buoy connected to the hydraulic cylinder.

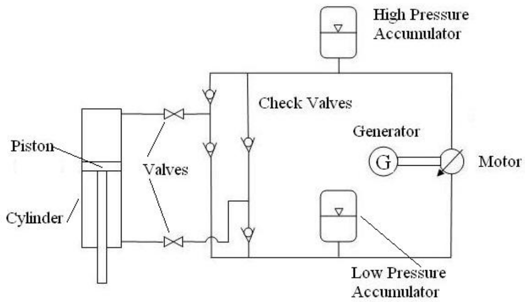

Figure 2: The hydraulic and generator system.

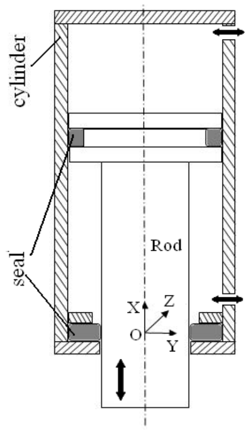

Figure 3: Sketch of the piston pump. Both the rod seal and the ring seal are shown in the figure.

2 Mathematical models for the wave energy converter system

A wave energy converter system consists of several sub-systems (i.e., mechanical, hydraulic and electrical systems) where energy is converted between different physical domains as it is transported through the system. In order to study the dynamic properties of this system, a mathematical model maybe used. The bond graph modelling language provides a useful and effective tool to derive such models. It is a unified approach which can represent both the linear and nonlinear systems equally well. A bond graph model can be constructed intuitively by considering energy flows between the ports of the system components. In addition, algebraic loops can be detected and avoided. Due to the features of the bond graph language, it has been used by Hals [6] and Engja [7] for modelling the WEC system. In this work, we will also follow this way to simulate the energy converter system. The goal of using this model is to get sufficient information for the wear calculation.

2.1 Heaving buoy

As seen in Fig. 1, the semi-submerged buoy is axisymmetric and can be described as a point absorber when it is small compared to the wavelength. We consider that the point absorber is constrained to move in heave mode only. Here we assume the hydro dynamic excitation and radiation forces, as well as the hydrostatic stiffness forces of the absorber, to be linear. Additionally, we assume that the platform is fixed.

The equation for single mode of motion for an absorber with mass M in time domain is given by Cummins [8]:

$$(M+m_\infty)\ddot{X}+\int_0^t K(t-\tau)\dot{X}(\tau)d\tau+CX = F_{exc}(t)+F_{ext}(X,\dot{X},t) \quad (1)$$

where m_∞ is the added mass at infinite frequency, C is the restoring coefficient, F_{exc} is the exciting force and F_{ext} is the external force, respectively. The retardation function $K(t\text{-}\tau)$ is related to the radiation damping, which may be seen as a fluid memory effect. It can be expressed as:

$$K(t)=\frac{2}{\pi}\int_0^\infty B(\omega)\cos(\omega t)d\omega = -\frac{2}{\pi}\int_0^\infty \omega\left[m(\omega)-m_\infty\right]\sin(\omega t)d\omega \quad (2)$$

where $B(\omega)$ is the wave damping coefficient and $m(\omega)$ is the added mass of the buoy. With the assumption of linearity, the convolution integral in Eq. (1) can be approximated by a state-space model [9]:

$$\dot{\mathbf{z}}(t)=\tilde{\mathbf{A}}\mathbf{z}(t)+\tilde{\mathbf{B}}\dot{X}(t) \quad \text{with} \quad \mathbf{z}(0)=\mathbf{0} \quad (3)$$

The radiation force $F_R(t)$ can be written as:

$$F_R(t)=\int_{-\infty}^t K(t-\tau)\dot{X}(\tau)d\tau \approx \tilde{\mathbf{C}}\mathbf{z(t)}+\tilde{\mathbf{D}}\dot{X}(t) \quad (4)$$

where $\mathbf{z}(t)=\left[z_1(t),z_2(t)\cdots,z_n(t)\right]^T$ is the state vector of the radiation force approximation.

2.2 Hydraulic system

The hydraulic system, as shown in Fig. 2 consists of an axial hydraulic pump with the piston rod connected to the heaving buoy, valves, low and high pressure accumulators and pipes. A mathematical model for each component is described in detail below.

The Hydraulic Cylinder: The oil in this system is lightly compressible and the pressure in the fluid will increase when the oil is compressed. This means that the density ρ is a function of the pressure P. The relation between the differential $d\rho$ in density and dP in pressure is given by the bulk modulus β [10]:

$$\frac{d\rho}{\rho}=\frac{dP}{\beta} \quad (5)$$

The mass balance for a volume V can be expressed as:

$$\frac{d}{dt}(\rho V)=\rho\dot{Q}_{net} \quad (6)$$

where $\dot{Q}_{net}$ is the net flow rate and is positive when the fluid flows into the volume. Here assume that the density is only time dependent. This leads to:

$$\dot{\rho}V+\rho\dot{V}=\rho\dot{Q}_{net} \quad (7)$$

The mass balance of a hydraulic volume V is obtained by combining Eq. (5) and Eq. (7), to give:

$$\dot{P}=\beta\frac{\dot{Q}_{net}-\dot{V}}{V} \quad (8)$$

By integrating Eq. (8) for both sides from time t_0 to t, we can get the pressure-volume equation which can be used for the hydraulic cylinder in our system:

$$P(t)=P(t_0)+\beta\int_{t_0}^{t}\frac{\dot{Q}_{net}-\dot{V}}{V}dt \quad (9)$$

The cylinder can be considered as a fluid capacitor which imposes a relationship between a pressure and the integral of the flow rate as shown in Eq. (9). We can use a two-port C-element to represent this cylinder component in the bond graph model.

Friction Force: The friction force between the cylinder and the piston is simulated as a function of relative velocity and pressure. It is assumed to be the sum of the Stribeck, Coulomb, Viscous and Static components. The friction model supplied by the library of the software 20-SIM [11] for the piston and cylinder is adopted,

$$F_f = F_n\times\{\mu_c+[\mu_s\times\left|\tanh(k\cdot v)\right|-\mu_c] \times\exp[-(\frac{v}{v_{st}})^2]\}\times\text{sign}(v)+F_n\cdot\mu_v\cdot v \quad (10)$$

where F_n is the normal force. It consists of the preload force, caused by the seal squeeze during the assembly, and the force proportional to the sealed pressure. Furthermore, μ_c, μ_s, μ_v and v_{st} are the Coulomb friction coefficient, static friction coefficient, viscous friction coefficient and characteristic Stribeck velocity, respectively. The friction can be represented as an R-element in the bond graph model which relates the force to the relative velocity between the cylinder and the piston.

Valves: Valves are used to control the direction of the flow and can be considered as resistances which cause pressure drop across them. Given the pressure drop, the flow can usually be calculated by the orifice equation derived from Bernoulli's energy equation for an incompressible steady-state flow [12]:

$$\dot{Q}=c_d\cdot A_{val}\sqrt{\frac{2}{\rho}\cdot\left|\Delta P\right|}\cdot\text{sign}(\Delta P) \quad (11)$$

where A_{val} is the cross section area of the valve, ρ is the density of the hydraulic oil, and ΔP is the pressure drop across the valve. Furthermore, c_d is the discharge coefficient which accounts for the energy losses. It depends on the geometry of the restriction and the Reynolds number R which characterizes the mode of the flow. The square root characteristic of Eq. (11) may cause numerical problems due to the fact that the derivative of the flow with regard to the pressure drop tends to infinity as the pressure drop approaches zero.

Borutzky and et al [13] proposed a single empirical flow formula for the valves. The model started from an approximation of the measured characteristic of the discharge coefficient c_d versus the square root of the Reynolds number $\sqrt{R}$ given by Merritt [14]. The equation is

$$\dot{Q} = \left(c_{turb} A_{val} \cdot \sqrt{\frac{2}{\rho}|\Delta P| + (\frac{\eta \cdot R_t}{2 \cdot c_{turb} \cdot D_{val}})^2} - A_{val} \cdot \eta \cdot \frac{R_t}{2 \cdot D_{val}} \right) \cdot \mathrm{sign}(\Delta P) \tag{12}$$

where c_{turb} is the discharge coefficient for turbulent flow, D_{val} is the diameter of the valve, η is the kinematic viscosity of the flow. Eq. (12) provides a linear relation for small pressure differences and the conventional square root law for turbulent conditions, and R_t is the Reynolds number at which the linear characteristic intersects with the constant value of c_{turb}. The transition from the laminar to the turbulent region is smooth. Fig. 4 compares the pressure-flow rate curves by using Eq. (11) and Eq. (12) with the same parameters. From the figure we can see there is a little deviation between the two curves. Energy losses of Eq. (12) are somewhat over-estimated, numerical difficulties during simulation are avoided since the slope of the $\dot{Q}/\Delta P$ is finite at zero pressure difference. In this work, we choose the empirical formula as the orifice model. It is easily used in bond graph models as an R-element.

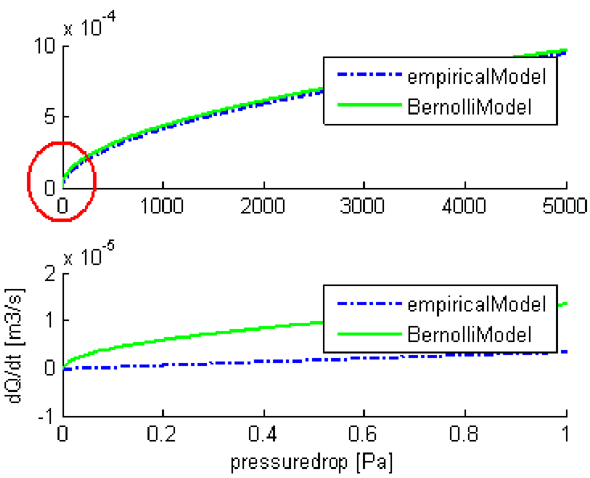

Figure 4: The relation between the pressure drop ΔP and the flow rate Q. The blue dashdot line corresponds to Eq. (12), the green solid one to Eq. (11). $c_d = 0.6$, $R_t = 10$, $D_{val} = 0.02$ m for the governing equations. The bottom figure is related to the red elliptical domain in the top figure with large scale.

Pressure Accumulators: The system contains one high-pressure accumulator and one low-pressure accumulator. Both of them are gas compressed bladders with a precharged pressure and they are used to reduce pressure peaks in the system and to store energy. The fluid flow (compared the gas, the fluid here is assumed to be incompressible), $\dot{Q}$, compresses the gas in the bladder, and the volume of the compressed gas determines the pressure in the accumulator. Here assuming that the peaks in the flow into or out of the accumulator are short in time, the gas does not have time to exchange much heat with its surroundings. Then the isentropic pressure-volume law

$$PV^{\gamma} = P_0 V_0^{\gamma} = \text{constant} \tag{13}$$

is a good approximation [12]. In this equation, γ is the ratio of the specific heat at constant pressure and volume (for air at atmospheric pressure, $\gamma \approx 1.4$). P and V are the instantaneous pressure and volume of the gas, and P_0 and V_0 are the values at some initial time.

The gas volume at time t is

$$V(t) = V_0 - \int_0^t \dot{Q} dt \tag{14}$$

Here $\dot{Q}$ is positive for a flow into the bladder.

This means the nonlinear capacitance relation between P and V is

$$P = P_0 V_0^{\gamma} \Big/ (V_0 - \int_0^t \dot{Q} dt)^{\gamma} \tag{15}$$

In the bond graph model C-elements are used for both of the accumulators.

Hydraulic Motor and Generator: In the hydraulic motor, the fluid of the hydraulic system flows into diving chambers in the motor, forcing a motor shaft to rotate with angular speed ω_m. The shaft is modeled with a small torsion compliance and connected to an electrical generator. In this paper, a motor model suggested by Pedersen [15] is adopted. However, the detailed motor model is not presented here. The generator is considered as a linear resistor, which dissipates the energy.

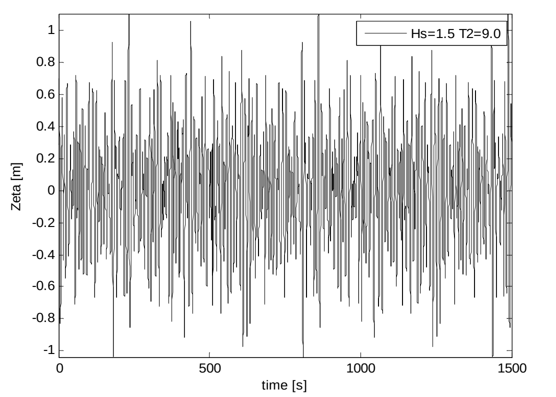

Figure 5: The wave elevation with H_s=1.5 m and T_2=9.0 s.

For oscillating absorbers with hydraulic power take-off, a series of experimental tests were performed in the ship model tank at MARINTEK in May 5th and 6th, 2004. Marré [1] verified his bond graph model to the experimental data in his master thesis. By introducing the governing equations mentioned above, the author has compared the model using a similar WEC system and parameters to the model which was developed by Marré [1] and got a relative good accordance between the two models.

In this work, the bond graphs have been implemented in the bond graph computer program 20-SIM. State-space equations based on the model are written by the computer program. A modified Pierson-Moskowitz (PM) spectrum with wave height H_s=1.5 m and mean wave period T_2=9.0 s was chosen to describe the sea state. The spectrum was discretized into 200 equally spaced ($\Delta\omega$=0.01 rad/s) sinusoidal harmonics in the range 0.25$\omega\leq\omega\leq$2.25 rad/s. The random phase angles are uniformly distributed between 0 and 2π and constant with time. The calculation has been carried out for a semi-submerged sphere of radius r=5 m, with mass $M=2.7\times10^5$ kg and added mass at infinite frequency $m_\infty=1.35\times10^5$ kg, which is equal to half the mass of the sphere. Fig. 5 shows the wave elevation in a time interval of 1500 s. The sample response is given for the period 200-1400 s, after excluding the transient start-up. The numerical simulation results for some chosen variables are shown in Fig. 6-8.

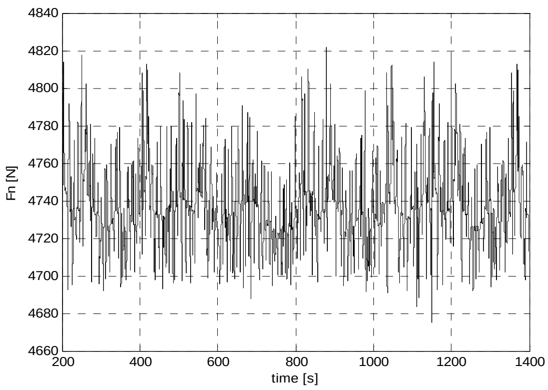

Figure 6: The interface force between the ring and cylinder.

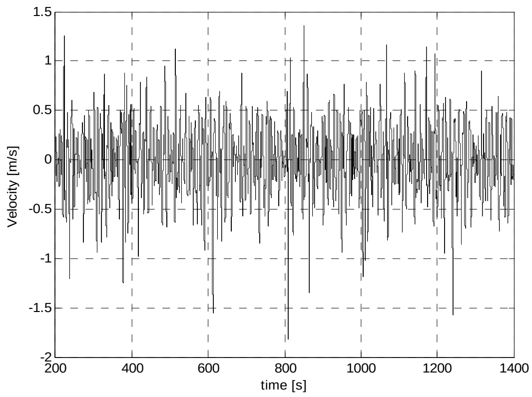

Figure 7: The relative velocity between the ring and the cylinder.

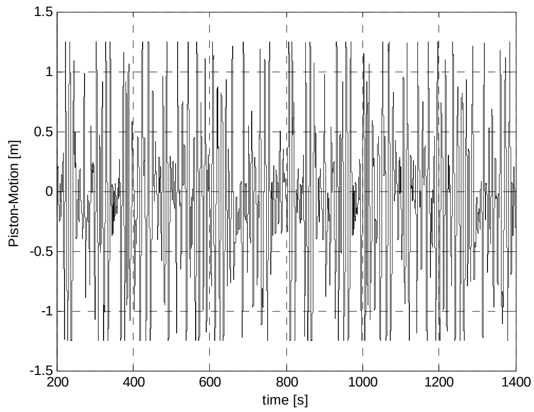

Figure 8: The ring motion in X direction. The coordinate system is set in Fig. 9.

3 Piston ring wear model

Abrasive wear is damage to a component surface that arises because of the motion relative to that surface of either harder asperities or perhaps hard particles trapped at the interface. The wear volume loss due to abrasion is usually expressed by using the Archard's equation as

$$V_w = K \cdot N \cdot x \tag{16}$$

where V_w is the wear volume, x is sliding distance, N is the normal force and K is the wear constant.

Considering the condition between the interface of the piston ring and cylinder system as shown in Fig. 9, a piston ring with width w and thickness d slides along a cylinder bore longitudinally in the X direction. Assuming that there is a uniformly distributed pressure p along the interface with the area A_{con}, the total normal load N can be calculated as

$$N = pA_{con} \tag{17}$$

The wear depth h of the ring can be obtained by using Eq. (16) and (17):

$$h = \frac{V_w}{A_{con}} = \frac{K \cdot N \cdot x}{A_{con}} = K \cdot p \cdot x \tag{18}$$

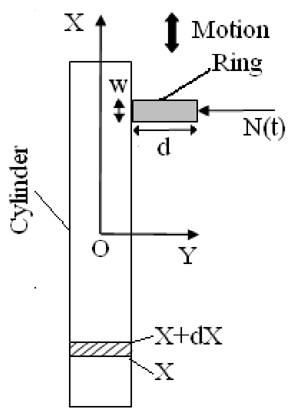

Figure 9: The coordinate system for the ring and cylinder.

Eq. (18) indicates that the process of the ring wear damage is proportional to the interface pressure p and the sliding distance x. For an irregular motion of the piston, the sliding distance x depends on the sequence of the local extremes. The sequence of local extremes is called the sequence of turning points. The travelled distance between the adjacent turning points is defined as the motion amplitude s. The time duration for finishing one amplitude is defined as a motion cycle, correspondingly. Here it is assumed that s can be described by its probability density function $f_s(s)$. The total number of cycles in the period T_w is N_T. The accumulated motion of the ring can then be expressed as:

$$x = \int_0^\infty N_T \cdot s \cdot f_s(s) ds = N_T \cdot E[s] \qquad (19)$$

where $E[s]$ is the mean value of the motion amplitude.

Introducing the mean frequency of the motion amplitude cycles, υ, Eq. (19) becomes:

$$x = \frac{N_T}{\upsilon} \cdot E[s] \cdot \upsilon = T_w \cdot E[s] \cdot \upsilon \qquad (20)$$

Substituting into Eq. (18) yields

$$h = K \cdot p \cdot E[s] \cdot \upsilon \cdot T_w \qquad (21)$$

If the term $K \cdot p \cdot E[s] \cdot \upsilon$ is independent of time t, it can be considered as the damage intensity, i.e. how much damage is accumulated per time unit. In that case, a simple predictor of the wear life time can be expressed as:

$$T_w = \frac{h}{K \cdot p \cdot E[s] \cdot \upsilon} \qquad (22)$$

The value of the wear constant K depends on various factors, such as the material properties, surface texture, particle size etc. If any of the factors are changed, the value of K would change too. Therefore, K needs to be determined experimentally for each case. Due to the absence of specific experimental values for the hydraulic system of the WEC, the value of K is chosen from literature on related applications [3-5]. In addition, K will also depend on the lubrication regime [4 and 16]. Visscher et al. [17] suggested that the wear constant decreases linearly as lubrication conditions changed from boundary lubrication to hydrodynamic lubrication. In the present analysis for the piston ring, only the boundary lubrication condition is considered, i.e., K is given a constant value during the calculation. The reason will be mentioned later in this paper.

4 Numerical Results

From the simulation results which are shown in Fig. 5-8, we can estimate the moments for the random dynamic response, which are shown in Table 1:

Random variables	Force N [N]	Velocity v [m/s]	Position X [m]
Mean	4737	0.2854	0.0485
Standard deviation	20.61	0.3526	0.5688
Coefficient of variation	0.0044	---	---
Skewness	---	---	0.1010
Kurtosis	---	---	4.162
Maximum	---	1.3639	---

Table 1: The random characters for the interface normal force N between the ring and cylinder, the relative velocity v and position X of the ring. ---: NaN

We can see that the coefficient of variation for the normal force is very small, i.e. 0.44 %. For simplification, the force here can be considered as constant value during the wear calculation, i.e. the interface pressure in Eq. (22) can be used as a constant. Fig. 7 shows that the maximum value of the piston velocity is 1.3639 m/s which is relatively small. Then the Sommerfeld number, which is proportional to the velocity, is also small. The lubrication regime here can be considered as the boundary conditions that are referred to in [18]. By counting the turning points of the ring motion in Fig. 8, the amplitude s for each cycle can be found. The sliding distance can be accumulated by all the amplitudes in a time interval. Fig. 10 shows the total distance that the piston moves. The relationship of the time and displacement is almost linear over the considered time scale, i.e., the average velocity is constant. Combining Eq. (20), the term $E[s]\cdot\upsilon$ has the unit of m/s, and can be considered as the average velocity v. The value is 0.28 m/s according to the fitting result shown in Fig. 10.

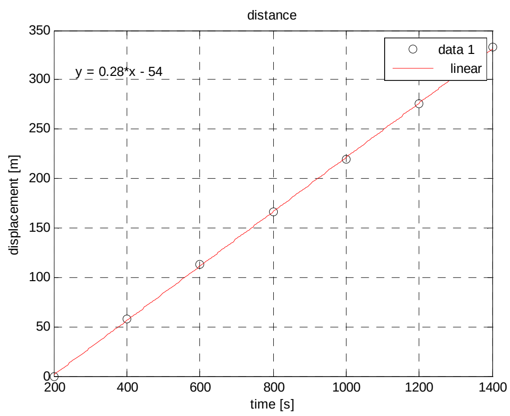

Figure 10: The displacement of the ring for time intervals of 200 s. The line is the linear fit based on the discrete values.

If the running-in process finishes at time t_0 with the wear depth h_0 for the ring, the total wear depth h at time t can be expressed as:

$$\begin{aligned} h &= h_0 + K \cdot p \cdot E[s] \cdot \upsilon \cdot (t - t_0) \\ &= h_0 + K \cdot p \cdot v \cdot (t - t_0) \end{aligned} \qquad (23)$$

From the reliability point of view, the failure time is a more relevant parameter. For the piston ring, in order to avoid pressure leakage, a warranty limit of the wear depth is set as h_{max}. According to Eq. (23), the time, t_{max}, to the condition that the wear exceeds the limit for leakage, is given by:

$$t_{\max} = \frac{\Delta h}{Kpv} + t_0 \Rightarrow for \quad \Delta h = h_{\max} - h_0 \tag{24}$$

where h_{max} is the maximum reduction before leak.

The wear constant K is chosen from literature [19], where some observed wear values in practice were supplied. Based on the analysis, a wear example for the ring is presented:

For an elastomeric ring with rectangular cross section, the parameters are set as: w=3.5×10^{-3} m, d=5.56×10^{-3} m, Δh=0.2×10^{-3} m, K=1×10^{-17} m^{2}N^{-1}, v=0.28 ms^{-1}, p=6.0×10^6 Pa, Rou=1 μm.

Substituting the parameters into Eq. (24), the maximum operation time for the ring is
t_{max}=3307 +t_0 [hours].

The result of the operation time for the case is only related to one sea state. For a real sea state, the parameters of the waves are random variables. So the response we've obtained here is conditional upon the parameters H_s and T_2. The unconditioned operation time can be calculated by considering different combinations of wave state variable values.

5 Conclusions

Table 1 shows that the estimated kurtosis of the ring position is about 4, so the process of the motion is non-normal. Therefore we can't consider the motion as a Gaussian process model due to the nonlinear equations and the latching control method used in the system during the simulation. It is a good choice to do the analysis in the time-domain by using the numerical simulation results. Fig. 10 indicates that the relationship between the time and piston displacement is linear. In the case of the short term period, the wave can be considered as a stationary process with a time independent mean elevation. It is reasonable to get a constant average velocity for the piston in a chosen sea state. Fig. 11 shows the spectrum of the wave and motion. It is found for the motion spectrum, there is a low-frequency effect. The reason is the check valves used in the converter system which will allow the piston to move only when the pressure in the cylinder is larger than that in the accumulators. If it is not, then the piston will wait until the pressure becomes large enough, and this will enlarge the motion period. The spectral peaks occur at 0.5522 (rad/s) for the wave and 0.5329 (rad/s) for the motion. Small deviation indicates that the response is consistent with the wave input.

In the real condition, the wear is influenced by a series of variables. Most of them are uncertain parameters. The wear phenomenon should be dealt with by probabilistic and statistical methods. In this paper, only the relative motion of the piston ring and cylinder is considered as a random process. Other parameters are considered as a certain value which is not the case in practice. How to consider these uncertainties in the wear model will be addressed in the further work. In addition, the wear constant K depends on various factors. How to develop an abrasive wear model by considering the effects of these factors will also be part of the future work.

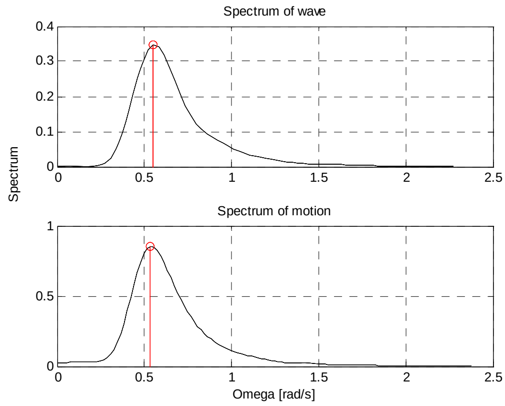

Figure 11: The spectrum of the wave (top) and ring motion (bottom).

Acknowledgements

Thanks to Professor Eilif Pedersen for valuable guidance. The authors also appreciate the financial support of the Norwegian Research Council which has been granted through Centre for Ships and Ocean Structures.

References

[1] I. R. Marré. *Modeling and simulation of a wave energy converter using a bond graph approach.* Master thesis, Norwegian University of Science and Technology, 2006.

[2] E. P. Becker and K. C. Ludema. A Qualitative Empirical Model of Cylinder Bore Wear. *Wear*, 225-229(Part I):387-404, 1999.

[3] B. H. Burr and K. M. Marshek. An equation for the abrasive wear of elastomeric O-ring materials. *Wear*, 81(2):347-356, 1982.

[4] A. Gangopadhyay. Development of a piston ring-cylinder bore wear model. CEC and SAE International 2000-01-1788.

[5] J. F. Archard and W. Hirst. The wear of metals under unlubricated conditions. Proceedings of the Royal Society of London, Series A, Mathematical and Physical Science, 236(1206): 397-410, 1956.

[6] J. Hals, R. Taghipour and T. Moan. Dynamics of a forcecompensated two-body wave energy converter in heave with hydraulic power take-off subject to phase control. In *Proc. 7th European Wave and Tidal Energy Conference,* Porto, Portugal, 2007.

[7] H. Engja and J. Hals. Modelling and simulation of sea wave power conversion systems. In *Proc. 7th European Wave and Tidal Energy Conference*, Porto, Portugal, 2007.

[8] W. Cummins. The impulse response function and ship motions. *Schiffstechnik* 9(1661): 101-109, 1962.

[9] R. Taghipour, T. Perez and T. Moan. Hybrid frequency time domain models for dynamic response analysis of marine structures. *Ocean Engineering*, 35:685-705, 2008.

[10] O. Egeland and J. T. Gravdahl. *Modeling and simulation for automatic Control*. Marine Cybernetics, 2002.

[11] 20-SIM, Controllab Products B.V., Drienerlolaan 5, HO-8266, 7522 NB Enschede, Netherlands.

[12] D. C. Karnopp, D. L. Margolis and R. C. Rosenberg. *System Dynamics: Modelling and Simulation of Mechatronic Systems*. John Wiley &Sons. 2006.

[13] W. Borutzky, B. Barnard and J. Thoma. An orifice flow model for laminar and turbulent conditions. *Simulation Modeling Practice and Theory*, 10(3-4):141-152, 2002.

[14] H. E. Merritt. *Hydraulic Control Systems*. John Wiley &Sons. 1967.

[15] E. Pedersen, Hydraulic motor model developed for 20-Sim. Norwegian University of Science and Technology. Unpublished.

[16] S. Tung and Y. Huang. Modeling of abrasive wear in a piston ring and engine cylinder bore system. *Tribology Transactions*, 47:17-22, 2004.

[17] M. Visscher, D. Dowson and C. M. Taylor. The profile Development of a twin-land oil-control ring during running-in. *Journal of Tribology*, 120(4):616-621, 1998.

[18] G. K. Nikas. Elastohydrodynamics and mechanics of rectangular elastomeric seals for reciprocating piston rods. *Journal of Tribology*, 125(1):60-69, 2003.

[19] H. J. Verbeek. Tribological Systems and Wear Factors. *Wear*, 56(1):81-92, 1979.